Innate Signaling Promotes Formation of Regulatory Nitric Oxide–Producing Dendritic Cells Limiting T-Cell Expansion in Experimental Autoimmune Myocarditis

Gabriela Kania, Stefanie Siegert, Silvia Behnke, Rafael Prados-Rosales, Arturo Casadevall, Thomas F. Lüscher, Sanjiv A. Luther, Manfred Kopf, Urs Eriksson and Przemyslaw Blyszczuk

The online version of this article, along with updated information and services, is located on the
World Wide Web at:
http://circ.ahajournals.org/content/127/23/2285

Data Supplement (unedited) at:
http://circ.ahajournals.org/content/suppl/2013/05/13/CIRCULATIONAHA.112.000434.DC1.html

Innate Signaling Promotes Formation of Regulatory Nitric Oxide–Producing Dendritic Cells Limiting T-Cell Expansion in Experimental Autoimmune Myocarditis

Gabriela Kania, PhD; Stefanie Siegert, PhD; Silvia Behnke, BSc; Rafael Prados-Rosales, PhD; Arturo Casadevall, PhD; Thomas F. Lüscher, MD; Sanjiv A. Luther, PhD; Manfred Kopf, PhD; Urs Eriksson, MD*; Przemyslaw Blyszczuk, PhD*

Background—Activation of innate pattern-recognition receptors promotes CD4+ T-cell–mediated autoimmune myocarditis and subsequent inflammatory cardiomyopathy. Mechanisms that counterregulate exaggerated heart-specific autoimmunity are poorly understood.

Methods and Results—Experimental autoimmune myocarditis was induced in BALB/c mice by immunization with α-myosin heavy chain peptide and complete Freund's adjuvant. Together with interferon-γ, heat-killed *Mycobacterium tuberculosis*, an essential component of complete Freund's adjuvant, converted CD11b^{hi}CD11c^{-} monocytes into tumor necrosis factor-α– and nitric oxide synthase 2–producing dendritic cells (TipDCs). Heat-killed *M. tuberculosis* stimulated production of nitric oxide synthase 2 via Toll-like receptor 2–mediated nuclear factor-κB activation. TipDCs limited antigen-specific T-cell expansion through nitric oxide synthase 2–dependent nitric oxide production. Moreover, they promoted nitric oxide synthase 2 production in hematopoietic and stromal cells in a paracrine manner. Consequently, nitric oxide synthase 2 production by both radiosensitive hematopoietic and radioresistant stromal cells prevented exacerbation of autoimmune myocarditis in vivo.

Conclusions—Innate Toll-like receptor 2 stimulation promotes formation of regulatory TipDCs, which confine autoreactive T-cell responses in experimental autoimmune myocarditis via nitric oxide. Therefore, activation of innate pattern-recognition receptors is critical not only for disease induction but also for counterregulatory mechanisms, protecting the heart from exaggerated autoimmunity.   (***Circulation***. 2013;127:2285-2294.)

Key Words: autoimmunity ■ immunology ■ myocarditis ■ nitric oxide

Inflammatory dilated cardiomyopathy refers to an end-stage heart failure phenotype that often results from myocarditis. Clinical observations and animal experiments suggest that infection-triggered autoimmunity plays an important role in myocarditis development and its progression to inflammatory dilated cardiomyopathy. Autoimmunity develops as a result of a breakdown in immunologic tolerance that leads to activation of self-reactive T lymphocytes. Heart-specific autoimmunity is a consequence of the lack of T-cell tolerance to heart-specific α-myosin heavy chain (α-MyHC) in mice and in humans.[1,2] Activation of pattern-recognition receptors on innate immune cells is widely believed to control the development of autoimmunity. Stimulation of Toll-like receptors (TLRs) on antigen-presenting cells (APCs) represents an essential step in activation and differentiation of autoreactive, naïve T cells into pathogenic, disease-mediating T helper (Th) cells.[3,4]

Editorial see p 2257
Clinical Perspective on p 2294

Commonly used animal models of autoimmune diseases are based on the delivery of self-antigen together with complete Freund's adjuvant (CFA), which contains heat-killed *Mycobacterium tuberculosis* (*Mtb*^{hk}) as its active component. In experimental autoimmune myocarditis (EAM), administration of α-MyHC peptide and CFA into BALB/c mice results in self-limiting, CD4+, Th cell–mediated heart-specific inflammation.[5–9]

Interferon-γ (IFN-γ)–producing Th1 cells represent a major subset of CD4+ T cells that infiltrate the myocardium in EAM; however, the role of Th1 cells and IFN-γ in pathogenesis of heart-specific autoimmunity is unclear. Mice lacking IFN-γ or its receptor are highly susceptible to EAM induced with α-MyHC/CFA.[10–12] In contrast, in a transgenic mouse model of spontaneous heart-specific autoimmunity, IFN-γ deficiency results in reduced myocarditis.[2]

Nitric oxide synthase (NOS) 2 represents an inducible isoform of NOS that is absent in healthy myocardium but has been clearly associated with tissue damage in patients with ischemic and nonischemic heart failure. In animal models, NOS2-producing cells have been reported to infiltrate the myocardium of α-MyHC/CFA–immunized mice[10] and on infection with Coxsackievirus[13] or *Trypanosoma cruzi*.[14] In EAM, NOS2 production entirely depends on IFN-γ.[10] NOS2-dependent nitric oxide has been shown to functionally eliminate heart-specific infections[15,16]; however, its definitive role in the regulation of infection-triggered heart-specific autoimmunity remains elusive.

NOS2 is produced by various cell types, including macrophages, activated monocytes, stromal fibroblastic cells, and endothelial cells. Tumor necrosis factor-α (TNF-α)– and NOS2–producing dendritic cells (TipDCs) represent another cell subset that is capable of producing nitric oxide.[17,18] TipDCs originate from monocytes and therefore belong to a subset of monocyte-derived dendritic cells (DCs). In contrast to conventional DCs, monocyte-derived DCs readily accumulate during infections and inflammation.[19] Both conventional and monocyte-derived DCs express CD11c and major histocompatibility complex class II and are effective antigen presenters, but they can be distinguished by CD64 antigen expression.[19] Monocyte-derived TipDCs have been reported to mediate the innate immune defense against bacterial infections.[17] Their role in the regulation of adaptive immune responses remains unclear.

Here, we show how TLR2 activation together with IFN-γ signaling converts monocytes into TipDCs that limit T-cell expansion and EAM development through nitric oxide. The present study reveals a novel principle of how cooperation of innate and adaptive mechanisms confines autoreactive heart-specific T-cell responses.

Methods

Mice
BALB/c mice (n=86) and *Rag2*−/− (n=39), *Ifng*−/− (n=15), *Ifngr1*−/− (n=9), *Myd88*−/− (n=4), *Nos2*−/− (n=44), and DO11.10-*tg* (n=20) mice on BALB/c background were described previously.[7,10,11,20,21] *Rag2*−/−*Ifngr1*−/− mice (n=15) were created by crossing *Rag2*−/− and *Ifngr1*−/− mice. In the respective in vitro experiments, cells were isolated from C57BL/6 mice (n=8) and *Tlr2*−/− (n=12), CD45.1-*tg*, (n=4), OT-II-*tg* (n=8), and *Nos2*−/− (n=4) mice on C57BL/6 background (all originally from The Jackson Laboratory, Bar Harbor, ME). Animal experiments were performed in accordance with Swiss federal law and were approved by local authorities.

EAM Induction
To induce EAM, mice were injected subcutaneously with 150 µg of α-MyHC (Ac-RSLKLMATLFSTYASADR-OH; Caslo) peptide emulsified 1:1 with CFA (BD Difco) on days 0 and 7. In the respective experiments, mice were injected with 150 µg of α-MyHC peptide emulsified 1:1 with incomplete Freund's adjuvant (IFA; BD Difco).

Chimeric Mice
Bone Marrow Chimeras
Six- to 8-week-old mice were lethally irradiated with 2 doses of 6.5 Gy as described[7] and transplanted with a total of 2×10⁷ crude donor bone marrow cells and used 6 weeks after bone marrow reconstitution.

Rag2−/− Chimeras
Six- to 8-week-old *Rag2*−/− or *Rag2*−/−*Ifngr1*−/− mice received a total of 10⁷ naïve splenocytes and were used 3 weeks after cell transfer.

Histopathology and Immunocytochemistry
Tissues were fixed in formalin or HOPE (HEPES–glutamic acid buffer–mediated organic solvent protection effect; DCS Innovative Diagnostic Systems) and embedded in paraffin. An antigen retrieval procedure was performed with ER2 buffer (Leica Biosystems), and sections were stained with rat anti-mouse CD45 (BD Bioscience), rabbit anti-mouse CD3 (NeoMarkers), rabbit anti-NOS2 (EMD Millipore), and rabbit anti-rat IgG (Abcam) antibodies and the Bond polymer refine detection kit using the Bond-Max system (both from Leica). Immunopositive cells were quantified with analySIS FIVE software (Olympus Australia). For nuclear factor-κB (NF-κB) p65 translocation, cells were stimulated for 30 minutes, fixed with 4% paraformaldehyde, permeabilized with 0.5% saponin (both from Sigma), and stained with rabbit anti-NF-κB p65 (Abcam) and AlexaFluor488 anti-rabbit IgG (Invitrogen).

[³H]-Thymidine Proliferation Assay
CD4+ T-cell magnetic beads (Miltenyi Biotec) were used to purify CD4+ T cells. A CD4− population was used as APCs. A total of 5×10⁴ CD4+ T cells cocultured with 10⁵ irradiated (25 Gy) syngeneic APCs were restimulated for 48 hours in the presence of serial dilutions of the α-MyHC peptide. Proliferation was assessed by measuring [³H]-thymidine incorporation during the last 8 to 16 hours.

Flow Cytometry and Fluorescence-Activated Cell Sorting
Single-cell suspensions were prepared from digested hearts treated with 0.2 mg/mL Liberase (Roche) for 45 minutes, lymph nodes treated with 3 mg/mL collagenase D and 1 mg/mL DNase (both from Sigma) for 30 minutes, and cultured cells with 70- and 40-µm cell strainers. Cells were incubated with the appropriate combination of fluorochrome-conjugated antibodies (online-only Data Supplement). Samples were analyzed with a FACSCanto analyzer (BD Bioscience) and FlowJo software (Tree Star). A proliferation index (number of divisions of dividing cells) of cells labeled with carboxyfluorescein succinimidyl ester was computed with FlowJo software. In the respective experiments, cells were sorted with FACSAria III (BD Bioscience).

Enzyme-Linked Immunosorbent Assay
Protein levels in supernatants were measured with mouse NOS2 (EIAab) and mouse TNF-α (BD Bioscience) enzyme-linked immunosorbent assay kits.

Quantitative Reverse-Transcription Polymerase Chain Reaction
RNA was isolated with RNeasy Plus Kits (Qiagen), and cDNA was amplified with the Power SYBR Green PCR Master Mix (Applied Biosystems). *Nos2* was detected with 5′-cagctgggctgtacaaacctt-3′ and 5′-tgaatgtgatgtttgcttcgg-3′ oligonucleotides. *Gapdh* levels were used for normalization.

Nitric Oxide Measurement

Concentrations of nitrite (NO_2^-) levels reflecting nitric oxide production were measured with the Griess reagent system (Promega).

Cell Cultures

A description of cell cultures is available in the online-only Data Supplement.

Statistical Analysis

Normally distributed data were analyzed by unpaired, 2-tailed Student t test and by 1-way ANOVA followed by Bonferroni post hoc test. All analyses were computed with GraphPad Prism 5 software. Differences were considered statistically significant for $P<0.05$ (for multiple comparisons adjusted with the Bonferroni correction).

Results

IFN-γ Signaling on Nonlymphocytes Limits T-Cell Expansion in EAM

Previous studies reported that IFN-γ– and IFN-γ receptor (IFN-γR)–deficient mice immunized with α-MyHC/CFA developed exacerbated myocarditis, postinflammatory fibrosis, and cardiac dysfunction,[10–12] which indicates IFN-γ priming, expansion, or differentiation of Th cells in EAM. Indeed, in hearts of IFN-γ–deficient ($Ifng^{-/-}$) mice, we observed an increased number of CD45+ cells (Figure 1A) and CD3+ T lymphocytes (Figure 1B), which peaked at day 16 of EAM. Restimulation of wild-type or $Ifng^{-/-}$ CD4+ T splenocytes with α-MyHC peptide in the presence of wild-type or $Ifngr1^{-/-}$ APCs showed that IFN-γ production by T cells suppressed their proliferation indirectly through IFN-γR signaling in APCs (Figures 1C and 1D). These data suggest that the exaggerated autoimmunity of $Ifng^{-/-}$ mice is not caused by intrinsic CD4+ T-cell hyperproliferation.

To verify this finding in vivo, we used a model of $Rag2^{-/-}$ mice (lacking T and B cells) injected with donor naïve splenocytes, which restored T and B subsets in $Rag2^{-/-}$ mice but did not contribute to other hematopoietic compartments (Figure I in the online-only Data Supplement). Accordingly, we generated mixed chimera by adoptive transfer of a mixture of CD45.1+ wild-type and CD45.2+$Ifngr1^{-/-}$ splenocytes into $Rag2^{-/-}$ mice 3 weeks before α-MyHC/CFA immunization. In these mice, all CD3+CD4+ T cells derived from donor splenocytes. At day 16 of EAM, we observed an unchanged CD45.1+-CD45.2+ T cell ratio in the spleen and inflamed hearts (Figure 1E), which indicates comparable expansion of autoimmune α-MyHC–specific wild-type and $Ifngr1^{-/-}$ CD4+ T cells. Moreover, $Rag2^{-/-}$ mice reconstituted with either wild-type or $Ifngr1^{-/-}$ cells showed comparable cardiac infiltrations with inflammatory CD45+ (Figure 1F) and CD3+ (Figure 1G) cells after α-MyHC/CFA immunization. In contrast, increased myocarditis was observed in $Rag2^{-/-}Ifngr1^{-/-}$ relative to $Rag2^{-/-}$ mice reconstituted with wild-type splenocytes before immunization (Figures 1H and 1I). Thus, the present results unequivocally demonstrate that IFN-γR signaling in the nonlymphocytic compartment controls T-cell expansion in α-MyHC/CFA–immunized mice.

Heat-Killed *M. Tuberculosis* Activates TLR2 to Induce IFN-γ–Dependent Nitric Oxide Production

Next, we studied how IFN-γ regulates T-cell expansion in the immune system. DO11.10-*tg* and OT-II-*tg* mice express
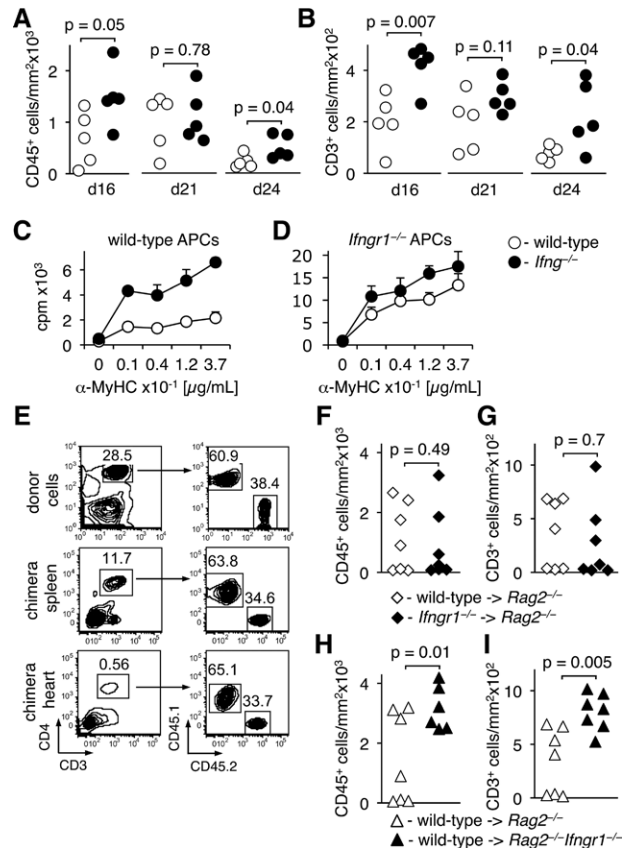
Figure 1. Interferon-γ (IFN-γ) signaling on nonlymphocytes controls development of experimental autoimmune myocarditis. **A** and **B**, Quantification of CD45+ (**A**) and CD3+ (**B**) immunopositive cells in heart sections of wild-type (white) and *Ifng*−/− (black) mice immunized with α-myosin heavy chain peptide and complete Freund's adjuvant (α-MyHC/CFA) at the indicated stages of experimental autoimmune myocarditis. **C** and **D**, Splenic CD4+ T cells from wild-type (white) and *Ifng*−/− (black) mice at day 21 of experimental autoimmune myocarditis were restimulated with α-MyHC peptide in the presence of wild-type (**C**) or *Ifngr1*−/− (**D**) antigen-presenting cells (APCs) for 48 hours. Incorporation of [3H]-thymidine indicates cell proliferation. Mean±SD, n=3; data are representative of 3 to 4 independent experiments. **E**, Wild-type (CD45.1+) and *Ifngr1*−/− (CD45.2+) splenocytes were mixed and transferred into *Rag2*−/− mice. After 3 weeks, the mixed chimeric mice were immunized with α-MyHC/CFA. Flow cytometric analysis of CD45.1 and CD45.2 alloantigens (**right**) gated on CD3+CD4+ T cells (**left**) shows donor cells used for injection (**top**) and splenocytes (**middle**) and heart inflammatory cells (**bottom**) of the mixed chimeras at day 16 of experimental autoimmune myocarditis. Numbers indicate percentage of cells in the adjacent gates. Representative plots of 4 to 8 independent mice. **F** and **G**, Quantification of CD45 (**F**) and CD3 (**G**) immunopositive cells on heart sections of α-MyHC/CFA–immunized *Rag2*−/− mice reconstituted with wild-type (white diamonds) or *Ifngr1*−/− (black diamonds) splenocytes. **H** and **I**, Quantification of CD45 (**H**) and CD3 (**I**) immunopositive cells on heart sections of α-MyHC/CFA–immunized *Rag2*−/− (white triangles) and *Rag2*−/−*Ifngr1*−/− (black triangles) mice reconstituted with wild-type splenocytes. P values computed with Student t test.

transgenic T-cell receptor that recognizes a peptide from chicken ovalbumin (OVA). We isolated CD4+ T cells from DO11.10-*tg* mice and injected them into $Rag2^{-/-}$ or $Rag2^{-/-}Ifngr1^{-/-}$ mice treated with IFA or CFA with or without OVA peptide. In agreement with the data above, DO11.10-*tg* CD4+ T cells showed much greater antigen-specific proliferation in

the spleen of *Rag2⁻/⁻Ifngr1⁻/⁻* than *Rag2⁻/⁻* mice (Figure 2A). Notably, even antigen-unspecific proliferation was enhanced in *Rag2⁻/⁻Ifngr1⁻/⁻* mice treated with CFA.

CFA, in contrast to IFA, contains heat-killed *M. tuberculosis* (*Mtb*ʰᵏ). To better understand the role of *Mtb*ʰᵏ in T-cell response, we isolated splenocytes from *Rag2⁻/⁻* and *Rag2⁻/⁻Ifngr1⁻/⁻* mice and cocultured them with CD4⁺ T cells from DO11.10-*tg* mouse in the presence or absence of *Mtb*ʰᵏ and OVA peptide. Interestingly, *Mtb*ʰᵏ potently inhibited CD4⁺ T-cell proliferation, which was dependent on intact IFN-γR signaling in APCs (Figure 2B). IFN-γ is known to regulate several metabolic pathways, including arginine metabolism and tryptophan catabolism, which control T-cell responses. N^G-nitro-l-arginine methyl ester, a competitive inhibitor of all NOS isoforms, greatly enhanced CD4⁺ T-cell proliferation in the presence of *Rag2⁻/⁻* (Figure 2C) but not *Rag2⁻/⁻Ifngr1⁻/⁻* (Figure 2E) splenic APCs, whereas no differences were observed by inhibition of arginase-1 and indoleamine 2,3-dioxygenase with the inhibitors $N^ω$-hydroxy-nor-arginine and 1-methyl-tryptophan, respectively. Accordingly, cocultures of CD4⁺ T cells and IFN-γR–competent splenocytes in the presence of N^G-nitro-l-arginine methyl ester,

but not $N^ω$-hydroxy-nor-arginine or 1-methyl-tryptophan, revealed reduced nitrite levels that reflected reduced nitric oxide production (Figures 2D and 2F). These results strongly suggest that T-cell proliferation is suppressed via IFN-γR–induced nitric oxide production by splenocytes. Consistently, we observed elevated nitrite levels in supernatants of proliferating CD4⁺ T cells in the presence of IFN-γR–sufficient but not IFN-γR–deficient splenocytes (Figure 2G). Importantly, although signaling from proliferating T cells was sufficient to induce nitric oxide production, the addition of *Mtb*ʰᵏ greatly enhanced it.

Furthermore, bacterial lipoproteins such as Pam3CSK4 and FSL-1 potently inhibited CD4⁺ T-cell proliferation and boosted nitric oxide production. In contrast, microbial nucleic acids such as polyinosinic-polycytidylic acid or ODN 1826 enhanced CD4⁺ T-cell proliferation and reduced nitrite levels (Figure II in the online-only Data Supplement).

Culture of *Rag2⁻/⁻* and *Rag2⁻/⁻Ifngr1⁻/⁻* splenocytes in the absence of T cells showed that stimulation with both IFN-γ and *Mtb*ʰᵏ was essential for upregulation of *Nos2* transcripts (Figure 2H), detectable NOS2 protein (Figure 2I), and elevated nitrite levels (Figure 2J) in the supernatant. Taken together,
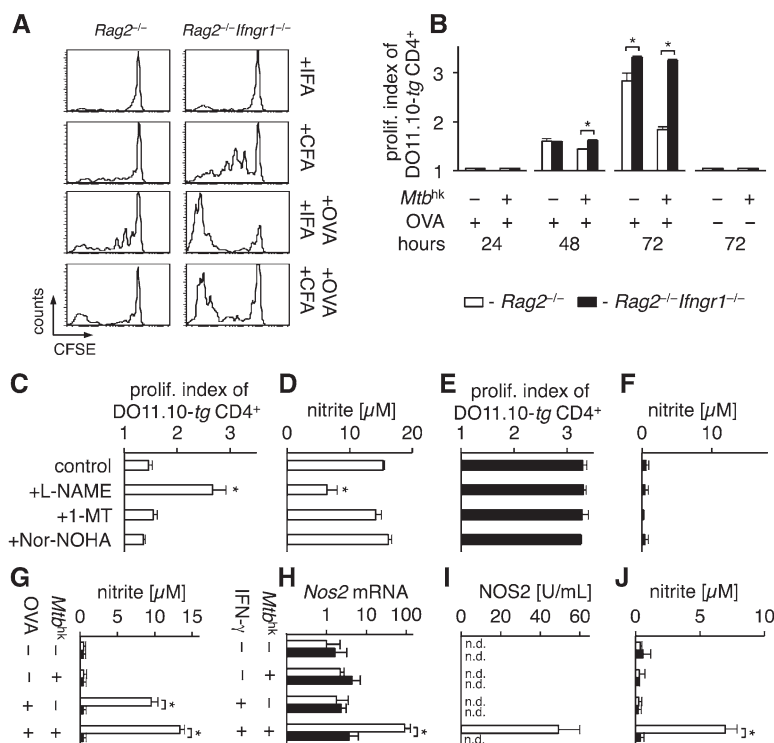
Figure 2. Heat-killed *Mycobacterium tuberculosis* (*Mtb*ʰᵏ) suppresses T-cell proliferation through interferon-γ receptor (IFN-γR)–dependent nitric oxide. **A**, Chicken ovalbumin (OVA)–specific CD4⁺ T cells (from DO11.10-*tg* mouse) were labeled with carboxyfluorescein succinimidyl ester (CFSE) and transferred to *Rag2⁻/⁻* and *Rag2⁻/⁻Ifngr1⁻/⁻* mice before treatment with incomplete Freund's adjuvant (IFA) or complete Freund's adjuvant (CFA) in the absence and presence of OVA peptide. Mice were analyzed 72 hours later. Histograms show CFSE dilutions of an individual representative of indicated groups of mice (n=3–4). **B**, Proliferation (prolif.) index (number of divisions of dividing cells) of CFSE-labeled DO11.10-*tg* CD4⁺ T cells (5×10⁴) cocultured with *Rag2⁻/⁻* (white) or *Rag2⁻/⁻Ifngr1⁻/⁻* (black) splenocytes (2×10⁵) in the presence or absence of 10 µg/mL *Mtb*ʰᵏ and 2 µg/mL OVA peptide. Data are representative of 3 independent experiments; mean±SD; n=3. *P<0.05 (Student *t* test). **C–F**, *Rag2⁻/⁻* (white; **C** and **D**) and *Rag2⁻/⁻Ifngr1⁻/⁻* (black; **E** and **F**) splenocytes were cocultured with CFSE-labeled DO11.10-*tg* CD4⁺ T cells (5×10⁴) in the presence of *Mtb*ʰᵏ and OVA peptide without (control) or with the following inhibitors: N^G-nitro-l-arginine methyl ester hydrochloride (L-NAME; 1 mmol/L), 1-methyl-tryptophan (1-MT; 5 µmol/L), or $N^ω$-hydroxy-nor-arginine (Nor-NOHA; 50 µmol/L). Proliferation of CFSE-labeled DO11.10-*tg* CD4⁺ T cells (**C** and **E**) and nitrite levels in supernatants (**D** and **F**) were analyzed after 72 hours. Mean±SD; *P<0.017 vs control (Student *t* test). **G**, Nitrite levels in supernatants of *Rag2⁻/⁻* (white) or *Rag2⁻/⁻Ifngr1⁻/⁻* (black) splenocytes and DO11.10-*tg* CD4⁺ T cells cocultured in the presence or absence of *Mtb*ʰᵏ and OVA peptide for 72 hours. **H–J**, *Rag2⁻/⁻* (white) or *Rag2⁻/⁻Ifngr1⁻/⁻* (black) splenocytes (2×10⁵) cultivated in the presence or absence of *Mtb*ʰᵏ and IFN-γ. Cells were analyzed for *Nos2* mRNA (**H**) and supernatants for nitric oxide synthase 2 (NOS2; **I**) and nitrite (**J**) after 72 hours. Mean±SD; *P<0.05 (Student *t* test). n.d. indicates not detected.

these data suggest that stimulation of myeloid cells with IFN-γ together with *Mtb*hk restrains CD4+ T-cell proliferation via nitric oxide production.

M. tuberculosis is recognized by immune cells primarily via TLR2, which induces the NF-κB signaling pathway. Using NF-κB–specific reporter cells, we showed that *Mtb*hk, as well as native membrane vesicles (MVs) produced by *M. tuberculosis* (*Mtb* MV), used TLR2 to activate NF-κB (Figure 3A and 3B). As expected, TNF-α activated the NF-κB pathway TLR2 independently (Figure 3A and 3B). *Mtb*hk or *Mtb* MV treatment of macrophages also induced nuclear translocation of NF-κB p65 (Figure 3C). Furthermore, macrophages treated with *Mtb*hk in the presence of IFN-γ showed TLR2-dependent nitric oxide (Figure 3D) and TNF-α (Figure 3E) production.

Next, we pretreated *Rag2*−/− splenocytes with the irreversible NF-κB inhibitor Bay 11-7082 (Sigma) and stimulated them with *Mtb*hk and IFN-γ. Bay 11-7082 completely prevented *Nos2* upregulation (Figure 3F) and nitric oxide production (Figure 3G). Furthermore, *Rag2*−/− splenocytes pretreated with Bay 11-7082 were unable to inhibit T-cell proliferation, consistent with the lack of nitric oxide production (Figure 3H and 3I). The present data demonstrate that *Mtb*hk requires TLR2 to induce NF-κB–dependent nitric oxide production.

M. Tuberculosis Antigens in Cooperation With IFN-γ Convert Monocytes Into Nitric Oxide–Producing Dendritic Cells

So far, it was unclear which cells produced nitric oxide in response to IFN-γ and *Mtb*hk stimulation. Analysis of intracellular NOS2 in *Rag2*−/− splenocytes pointed to CD11bhiCD11c+ cells as major nitric oxide producers (Figure 4A). CD11bhiCD11c+ cells, however, are present in low numbers only in spleens and lymph nodes of naïve mice (Figure 4B). We found that they developed readily from CD11bhiCD11c− monocytes when exposed to *Mtb*hk or IFN-γ (Figure 4C). In fact, stimulation of sorted CD11bhiCD11c− monocytes with IFN-γ or *Mtb*hk induced expression of CD11c and CD64, but costimulation with IFN-γ and *Mtb*hk or TNF-α was required to boost NOS2 (Figure 4C) and nitric oxide production (Figure 4D). Notably, IFN-γ and *Mtb*hk exerted distinct activities on CD11bhiCD11c− monocytes upregulating major histocompatibility complex class II (Figure 4C) and TNF-α production, respectively (Figure 4E). The present data showed that *Mtb*hk and IFN-γ converted CD11bhiCD11c− monocytes into TNF-α– and NOS2-producing DCs. This subset of DCs has been previously described and termed TipDCs.[17]

The present findings showed that *Mtb*hk-stimulated TipDCs massively produce TNF-α, which potentially could boost local NOS2 production. As shown above, *Mtb*hk is specifically recognized by TLR2, and therefore, stimulation with IFN-γ and *Mtb*hk resulted in impaired NOS2 production in CD11bhiCD11c− *Tlr2*−/− cells (Figure 4F). Instead, coculture with wild-type TipDCs boosted NOS2 production in *Tlr2*−/− cells (Figure 4G). This result clearly indicates that *Mtb*hk-activated TipDCs contribute to positive regulation of NOS2 in neighboring cells.

DCs are specialized in the capturing, processing, and presenting of antigens to T cells. We found that in contrast to
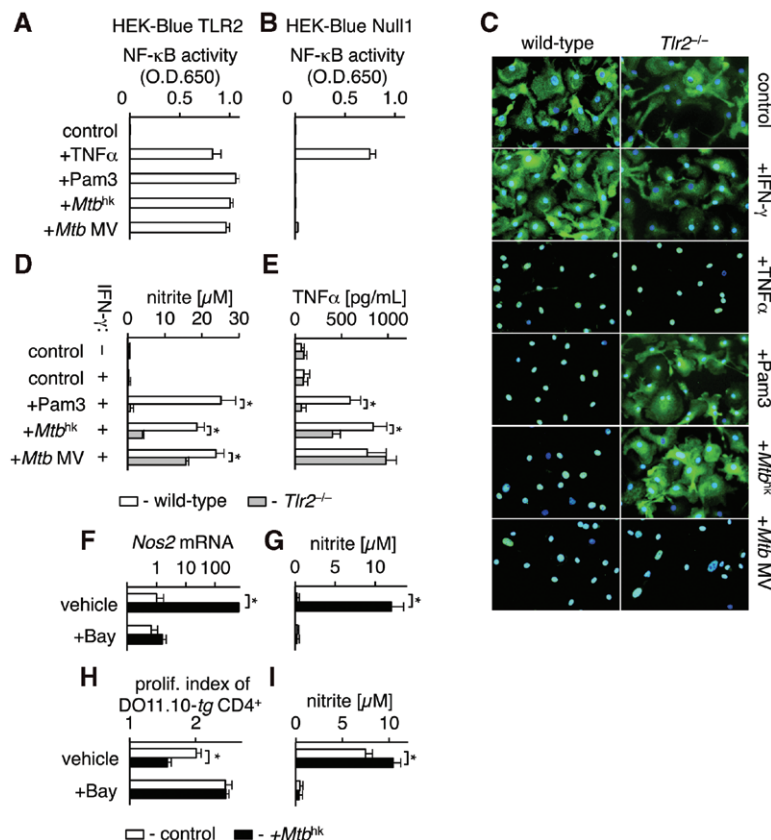
Figure 3. Nuclear factor-κB (NF-κB) pathway controls nitric oxide synthase 2 (NOS2)–dependent nitric oxide production. **A** and **B**, NF-κB activity measured in NF-κB reporter cells expressing Toll-like receptor 2 (HEK-Blue TLR2; **A**) or control (HEK-Blue Null1; **B**), unstimulated (control) and stimulated with 50 ng/mL tumor necrosis factor-α (TNF-α), 1 µg/mL Pam3CSK4, 10 µg/mL heat-killed *Mycobacterium tuberculosis* (*Mtb*hk), or 20 ng/mL *Mtb* membrane vesicles (MV). O.D. 650 indicates optical density at 650 nm. **C**, Representative immunofluorescence of NF-κB p65 (green) in nonstimulated (control) and stimulated (30 minutes) wild-type (**left**) and *Tlr2*−/− (**right**) bone marrow–derived macrophages. DAPI (blue) was used to stain nuclei; magnification ×200. **D** and **E**, Wild-type (white) and *Tlr2*−/− (gray) bone marrow–derived macrophages (5×10⁵) were cultured in the presence (+) or absence (−) of interferon-γ (IFN-γ) and stimulated with Pam3CSK4, *Mtb*hk, or *Mtb* MV. Cell supernatants were analyzed for nitrite (**D**) and TNF-α (**E**) after 72 hours. Mean±SD, *P<0.05 (Student *t* test). **F–I**, *Rag2*−/− splenocytes (2×10⁵) were pretreated (1 hour) with vehicle or the irreversible NF-κB inhibitor Bay 11-7082 (Bay). **F** and **G**, Pretreated cells were cultured in the presence of IFN-γ without (control) or with *Mtb*hk and analyzed for *Nos2* mRNA (**F**) and supernatants for nitrite (**G**) after 72 hours. **H** and **I**, Pretreated cells were cocultured with DO11.10-*tg* CD4+ T cells in the presence of chicken ovalbumin (OVA) peptide without (control) or with *Mtb*hk. Proliferation (Prolif.) of carboxyfluorescein succinimidyl ester (CFSE)–labeled DO11.10-*tg* CD4+ T cells (**H**) and nitrite levels in supernatants (**I**) were analyzed after 72 hours. Mean±SD, *P<0.05 (Student *t* test).
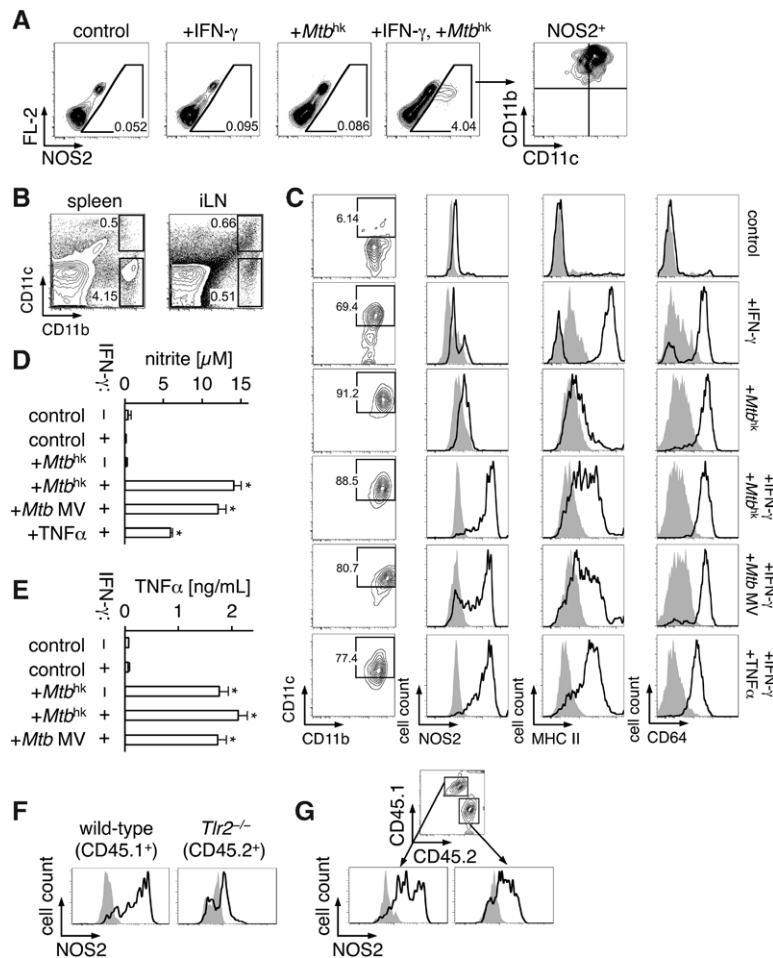
Figure 4. *Mycobacterium tuberculosis* antigens induce formation of nitric oxide synthase 2 (NOS2)–producing monocyte-derived dendritic cells. **A**, Representative flow cytometry analysis of intracellular NOS2 in *Rag2*–/– splenocytes cultivated in the absence (control) and presence of heat-killed *M. tuberculosis* (*Mtb*hk) or interferon-γ (IFN-γ), as indicated on top of the diagrams, for 72 hours. NOS2-positive cells were analyzed for CD11b and CD11c (**right**). Numbers indicate percentage of cells in the adjacent gates; FL-2, empty channel. Data are representative of 3 independent experiments. **B**, Representative flow cytometry dot plots of naïve splenocytes (**left**) and inguinal lymph node (iLN) cells (**right**) stained with anti-CD11c and anti-CD11b antibodies. Gated cells were sorted and used for further analysis. Value in gates indicates percentage. **C–E**, Sorted splenic CD11bhiCD11c– cells (gating in **B**; 5×10⁴) were cultured unstimulated (control) or in the presence of 50 ng/mL IFN-γ, 10 µg/mL *Mtb*hk, 20 ng/mL *Mtb* membrane vesicles (MV), or 50 ng/mL tumor necrosis factor-α (TNF-α) as indicated and were analyzed after 72 hours. Shown are representative dot plots of CD11b and CD11c expression and histograms of major histocompatibility complex class II (MHC II), CD64, and intracellular NOS2 (**C**). Value shows percentage of double-positive cells in the adjacent gate (dot plots). Isotype controls are shown in gray (histograms). Supernatants were analyzed for nitrite (**D**) and TNF-α (**E**). Mean±SD, n=4; *P<0.0125 vs control (Student t test). Data are representative of 3 independent experiments. **F** and **G**, CD11bhiCD11c– splenocytes (gating in **B**; 5×10⁴ cells) were sorted from wild-type (CD45.1+) and *Tlr2*–/– (CD45.2+) mice. Cells were cultured separately (**F**) or in cocultures (**G**) in the presence of IFN-γ and *Mtb*hk for 72 hours. Intracellular NOS2 was analyzed by flow cytometry on CD45.1+ (wild-type; **left**) and CD45.2+ (*Tlr2*–/–; **right**) gated cells. Data are representative of 3 independent experiments. Isotype controls are shown in gray.

CD11bhiCD11c– monocytes, naïve and *Mtb*hk/IFN-γ–activated CD11bhiCD11c+ DCs effectively induce antigen-specific T-cell proliferation (Figure 5A). This result indicates that monocytes converting to the DC phenotype acquire APC properties.

To date, definitive evidence that nitric oxide produced by TipDCs limits T-cell expansion is lacking. CD11bhiCD11c– cells with a disrupted *Ifngr1, MyD88* or *Tlr2* gene stimulated with IFN-γ and *Mtb*hk showed impaired *Nos2* expression (Figure 5B and 5F) and failed to produce nitric oxide (Figure 5C and 5G), which confirms that IFN-γR signaling and *Mtb*hk-induced TLR2/MyD88 signaling was crucial for development of nitric oxide–producing TipDCs. Next, we cocultured OVA-reactive CD4+ T cells with conventional DCs in the presence of CD11bhiCD11c– cells, OVA peptide, and *Mtb*hk. We observed uncontrolled T-cell proliferation (Figure 5D and 5H) and reduced nitric oxide (Figure 5E and 5I) in the presence of *Nos2*–/–, *Ifngr1*–/–, *MyD88*–/–, or *Tlr2*–/– monocyte-derived DCs. This result clearly demonstrates that NOS2 production defines the regulatory role of monocyte-derived DCs.

TipDCs Promote Nitric Oxide Production in Stromal Fibroblasts

Stromal cells represent another important source of NOS2-derived nitric oxide. We used the nitric oxide–producing pLN2 cell line established from lymph node fibroblasts to address whether *M. tuberculosis* antigens affect nitric oxide production in this cell type. However, stimulation with Pam3CSK4, *Mtb*hk, or *Mtb* MV failed to induce NF-κB p65 nuclear translocation on pLN2 cells, probably because of insufficient TLR2 expression (Figure 6A and 6B). Instead, TNF-α induced translocation of NF-κB p65 into nucleus (Figure 6A and 6B) and in cooperation with IFN-γ promoted *Nos2* expression and nitric oxide production in these fibroblasts (Figure 6C and 6D). Accordingly, addition of *Mtb*hk or *Mtb* MV to cocultures of pLN2 with conventional DCs and OT-II-*tg* CD4+ T cells failed to affect antigen-specific T-cell proliferation and nitric oxide levels (Figure 6E and 6F). Thus, these results demonstrate that TLR2 is required for *Mtb*hk-induced nitric oxide production not only in myeloid but also in stromal cells.

We demonstrated that *Mtb*hk induced production of cytokines, such as TNF-α, which could stimulate NOS2 production in monocyte-derived DCs and in pLN2 cells. To analyze whether TipDCs activated with *Mtb*hk could stimulate NOS2 production in stromal cells, we sorted CD11bhiCD11c– from *Nos2*–/– splenocytes and cocultured them with pLN2 cells in the presence or absence of *Mtb*hk. Addition of *Mtb*hk induced nitric oxide levels in cocultures (Figure 6G). Given that pLN2 cells fail to respond to *Mtb*hk, these results indicate that *Mtb*hk-activated TipDCs can induce nitric oxide production in stromal cells.
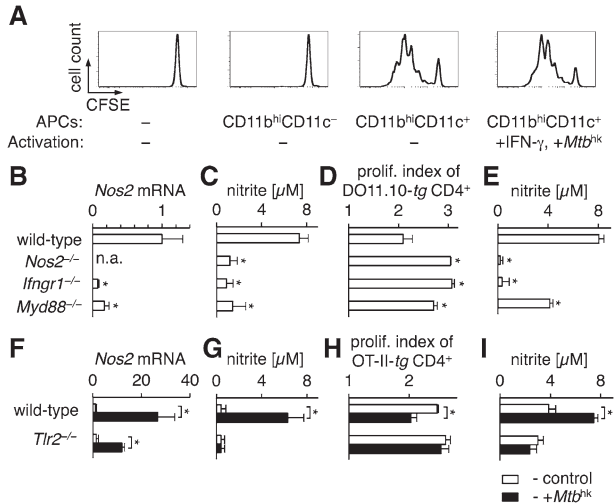
Figure 5. Monocyte-derived dendritic cells induce and limit T-cell proliferation. **A**, Splenocytes that were unactivated (–) or activated with interferon-γ (IFN-γ) and heat-killed *Mycobacterium tuberculosis* (*Mtb*hk) were cultured in the presence of chicken ovalbumin (OVA) peptide for 24 hours. Next, sorted CD11bhiCD11c− or CD11bhiCD11c+ cells (gating in Figure 4B) were used as antigen-presenting cells (APCs; 10⁴) in cocultures with carboxyfluorescein succinimidyl ester (CFSE)–labeled DO11.10-*tg* CD4+ T cells (5×10⁴) as indicated. Representative histograms show CFSE dilutions of DO11.10-*tg* CD4+ T cells after 72 hours. **B–E**, Sorted CD11bhiCD11c− cells (5×10⁴) from the indicated mouse strains were cultured in the presence of IFN-γ and *Mtb*hk for 72 hours and analyzed for *Nos2* mRNA (**B**) and supernatants for nitrite (**C**). Sorted CD11bhiCD11c− cells (5×10⁴) were cocultured with conventional dendritic cells (10⁴) and CFSE-labeled DO11.10-*tg* CD4+ T cells in the presence of *Mtb*hk and OVA peptide. Proliferation (prolif.) index of DO11.10-*tg* CD4+ T cells (**D**) and nitrite levels in supernatant (**E**) were analyzed after 72 hours. Data are representative of 2 independent experiments. Mean±SD, n=3, *P<0.017 vs wild-type (Student t test). n.a. indicates not analyzed. **F–I**, Sorted splenic CD11bhiCD11c− cells (5×10⁴) from wild-type (white) or *Tlr2−/−* (black) mice were cultured in the presence of IFN-γ without (control) or with *Mtb*hk and analyzed for *Nos2* mRNA (**F**) and supernatants for nitrite (**G**) after 72 hours. Sorted CD11bhiCD11c− cells (5×10⁴) were cocultured with conventional dendritic cells (10⁴) and CFSE-labeled OT-II-*tg* CD4+ T cells in the presence of OVA peptide without (control) or with *Mtb*hk. Proliferation index of OT-II-*tg* CD4+ T cells (**H**) and nitrite levels in supernatant (**I**) were analyzed after 72 hours. Data are representative of 2 independent experiments. Mean±SD, n=3 to 4; *P<0.05 (Student t test).

Nitric Oxide From TipDCs or Stromal Cells Limits EAM Progression

So far, the present data demonstrated that *Mtb*hk induced NOS2 and nitric oxide production in vitro. To analyze its role in EAM development, we subcutaneously injected mice with α-MyHC/CFA into the right groin and with α-MyHC/IFA into the left groin and 5 days later analyzed inguinal lymph nodes (Figure 7A). At the site of α-MyHC/CFA injection, inguinal lymph nodes were enlarged and contained more NOS2-producing cells (Figure 7B). Furthermore, CFA-primed inguinal lymph nodes were infiltrated by higher numbers of CD11bhiCD11c+ cells (Figure 7C), which showed enhanced NOS2 levels (Figure 7D). Stromal cells from the CFA- and IFA-primed inguinal lymph nodes showed comparable NOS2 production (Figure 7E). These results suggest that in the EAM model, *Mtb*hk promotes formation of TipDCs at the site of antigen delivery.

To address a direct role of NOS2 in EAM, we immunized BALB/c and *Nos2−/−* mice with α-MyHC/CFA. We observed
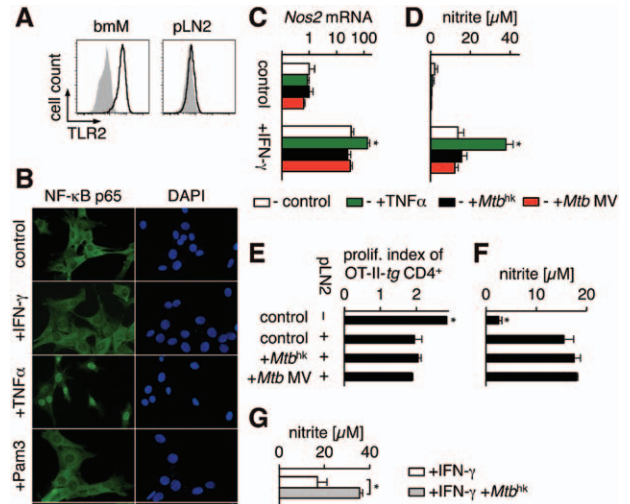
Figure 6. *Mycobacterium tuberculosis* antigens fail to regulate nitric oxide production in pLN2 stromal fibroblasts. **A**, Representative flow cytometry analysis of Toll-like receptor 2 (TLR2) in bone marrow macrophages (bmM; **left**) and pLN2 cells (**right**). Isotype controls are shown in gray. **B**, Nuclear translocation of nuclear factor-κB (NF-κB) p65 (green) in pLN2 cells. Cells were treated for 30 minutes without (control) or with 10 ng/mL interferon-γ (IFN-γ), 50 ng/mL tumor necrosis factor-α (TNF-α), 1 μg/mL Pam3CSK4, 10 μg/mL heat-killed *M tuberculosis* (*Mtb*hk), or 20 ng/mL *Mtb* membrane vesicles (MV). DAPI (blue) was used to stain nuclei; magnification ×200. Data are representative of 3 independent experiments. **C** and **D**, pLN2 cells were cultured in the absence (control) or presence (+IFN-γ) of IFN-γ and without (white) or with (green) TNF-α, *Mtb*hk (black), or *Mtb* MV (red) for 72 hours and analyzed for *Nos2* mRNA (**C**) and supernatants for nitrite (**D**). Mean±SD, n=4, *P<0.017 vs controls (white; Student t test). **E** and **F**, Conventional dendritic cells and OT-II-*tg* carboxyfluorescein succinimidyl ester (CFSE)–labeled CD4+ T cells were cocultured without (−) or with (+) pLN2 cells in the absence (control) or presence of *Mtb*hk or *Mtb* MV. Proliferation (prolif.) index of OT-II-*tg* CD4+ T cells (**E**) and nitrite levels in supernatants (**F**) are shown. Mean±SD, n=3, *P<0.017 vs control +pLN2 (Student t test). Data are representative of 3 independent experiments. **G**, Sorted CD11bhiCD11c− splenocytes (gating in Figure 4B) from *Nos2−/−* mice were cocultured with pLN2 cells in the presence of IFN-γ (white) or IFN-γ and *Mtb*hk (gray) for 72 hours and analyzed for nitrite in supernatants. Data are representative of 3 independent experiments. Mean±SD, n=3, *P<0.05 (Student t test).

enhanced myocarditis (Figure 8A and 8B) and an increased number of infiltrating CD45+ cells (Figure 8C) and CD3+ T lymphocytes (Figure 8D) in hearts of *Nos2−/−* mice at day 16 of EAM. We found that both CD11bhiCD11c− monocytes and CD11bhiCD11c+ monocyte–derived DCs heavily infiltrated the myocardium in EAM at this time point. As expected, NOS2 was identified mainly in the CD11bhiCD11c+ population that also expressed major histocompatibility complex class II and CD64 (Figure 8E), which indicates a TipDC phenotype. Furthermore, restimulation of wild-type and *Nos2−/−* CD4+ T cells with α-MyHC peptide presented by wild-type or *Nos2−/−* APCs showed that absence of NOS2 in APCs, but not in CD4+ T cells, resulted in enhanced α-MyHC–specific T-cell proliferation (Figure III in the online-only Data Supplement).
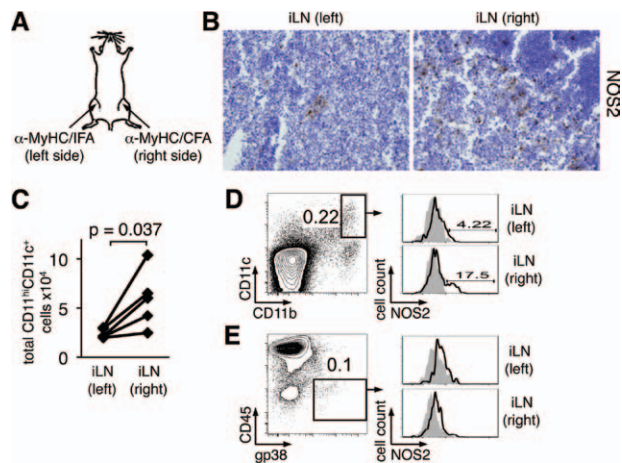
Figure 7. Heat-killed *Mycobacterium tuberculosis* (*Mtb*hk) in the adjuvant promotes formation of nitric oxide synthase 2 (NOS2)–positive monocyte-derived dendritic cells in experimental autoimmune myocarditis. BALB/c mice were subcutaneously immunized with α-myosin heavy chain peptide and complete Freund's adjuvant (α-MyHC/CFA) in the right groin and with α-MyHC/incomplete Freund's adjuvant (IFA) in the left groin (**A**), and inguinal lymph nodes (iLNs) were analyzed at day 5. **B**, Representative immunohistochemistry of NOS2 (brown) in the indicated iLN (magnification ×100). **C**, Quantification of total CD11b^{hi}CD11c$^+$ cells isolated from the indicated iLN. Lines link iLNs from the same mouse. *P* value computed with paired *t* test. **D** and **E**, Representative flow cytometry analysis of intracellular NOS2 in CD11b^{hi}CD11c$^+$ cells (**D**) and in CD45$^-$gp38$^+$ stromal cells (**E**) from the indicated iLN. Arrows show gating strategy. Numbers indicate percentage of cells in the adjacent gates. Isotype controls are shown in gray.

To verify that nitric oxide produced by inflammatory TipDCs prevented uncontrolled myocarditis, we generated crisscross bone marrow chimeras by injection of the whole bone marrow from wild-type or *Nos2*$^{-/-}$ mice to lethally irradiated wild-type and *Nos2*$^{-/-}$ recipients. Six weeks later, we immunized the bone marrow chimeric mice with α-MyHC/CFA to induce EAM. Interestingly, we found elevated numbers of infiltrating CD45$^+$ cells (Figure 8F) and CD3$^+$ T lymphocytes (Figure 8G) only in *Nos2*$^{-/-}$→*Nos2*$^{-/-}$ chimeras, which suggests that nitric oxide production by either radiosensitive hematopoietic cells or by radioresistant nonhematopoietic stromal cells was sufficient to prevent exacerbated myocarditis. Immunohistochemistry of NOS2 on heart tissue sections from the bone marrow chimeras showed NOS2-positive cells in both hematopoietic (wild-type→*Nos2*$^{-/-}$) and nonhematopoietic compartments (*Nos2*$^{-/-}$→wild-type; Figure 8H). As illustrated above, TipDCs represent major NOS2 producers in hematopoietic inflammatory fraction in EAM. Heart tissue analysis of *Nos2*$^{-/-}$→wild-type chimeras showed that NOS2 was expressed by gp38–positive fibroblasts in the inflamed heart (Figure IV in the online-only Data Supplement). Importantly, NOS2-producing radioresistant stromal cells were found only in the inflamed areas, which indicates local induction, and NOS2 was undetectable in healthy hearts.

Discussion

In myocarditis, IFN-γ–producing Th1 cells infiltrate the myocardium, but the role of IFN-γ remains unclear. IFN-γ is a proinflammatory cytokine, which when overexpressed induces chronic myocarditis.[22] Furthermore, in a transgenic model of spontaneous autoimmune myocarditis, IFN-γ was recognized

to promote inflammation.[2] On the other hand, IFN-γ clearly attenuates myocarditis induced with α-MyHC/CFA[10–12] or triggered by viral[23] or parasitic[24] infections. The present data showing increased EAM susceptibility of *Rag2*$^{-/-}$*Ifngr1*$^{-/-}$ chimeric mice reconstituted with wild-type lymphocytes clearly demonstrated that lack of the IFN-γ receptor on non-T cells was responsible for exacerbated T-cell expansion and myocarditis in the α-MyHC/CFA model. We identified the well-known IFN-γ–dependent nitric oxide production as the key mechanism limiting autoreactive T-cell proliferation in EAM.

Effective NOS2-dependent nitric oxide production requires coactivation of the NF-κB pathway with TLR agonists or proinflammatory cytokines such as TNF-α. Activated T cells produce both cosignals (IFN-γ and TNF-α) required for *Nos2* upregulation. Here, we showed that in addition to T cells, direct innate signaling on myeloid cells contributes remarkably to nitric oxide production. The present data demonstrate that *M. tuberculosis* antigens promoted conversion of CD11b^{hi}CD11c$^-$ monocytes into nitric oxide–producing TipDCs. Importantly, TipDCs represent a subset of monocyte-derived DCs that correspond to classically activated macrophages and are distinct from conventional DCs.[19,25] In line with previous findings,[19,25] we showed that TipDCs massively accumulate during inflammation. A previous report pointed to a proinflammatory role of monocyte-derived DCs in autoimmunity.[26] The present data show that monocyte-derived DCs express major histocompatibility complex class II and therefore can engage and also potentially expand autoreactive CD4$^+$ T cells. Importantly, the present data clearly show that nitric oxide produced by TipDCs efficiently suppresses T-cell expansion. Therefore, it is important to distinguish TipDCs from other NOS2-negative monocyte-derived DCs because of the opposing effects of these two DC subsets on T-cell proliferation. Although the ultimate role of monocyte-derived DCs and TipDCs in autoimmunity has not been fully elucidated yet, the present data clearly demonstrate that NOS2 production defines their regulatory function.

Subcutaneous delivery of self-peptides together with CFA represents the most common immunization procedure in rodent models of autoimmune diseases. The presence of *Mtb*hk in CFA is critical for the induction of pathogenic T-cell response in these models.[3] The innate immune response apparently plays a dual role in regulating adaptive autoimmunity. On one hand, it promotes development of pathogenic Th cells and inflammation. On the other hand, together with IFN-γ, it prevents uncontrolled expansion of activated T cells.

Experiments with bone marrow chimeras showed that in EAM, both hematopoietic and stromal cells produced functional NOS2. We showed that *Mtb*hk-activated TipDCs promote nitric oxide production in stromal fibroblasts, which failed to directly respond to *Mtb*hk because of the absence of TLR2 expression. Thus, we propose that both T cells and TipDCs regulate NOS2 production in stromal cells. The present data suggest that this mechanism is not limited to the lymphatic system. In fact, T cells and TipDCs infiltrate the heart in EAM, and NOS2 is detected in gp38–positive cardiac fibroblasts only within the inflamed myocardium. Of note, paracrine NOS2 regulation by TipDCs is not restricted to stromal cells. The present data clearly show that *Mtb*hk-activated TipDCs promote NOS2 production in other monocyte-derived cells. Thus,
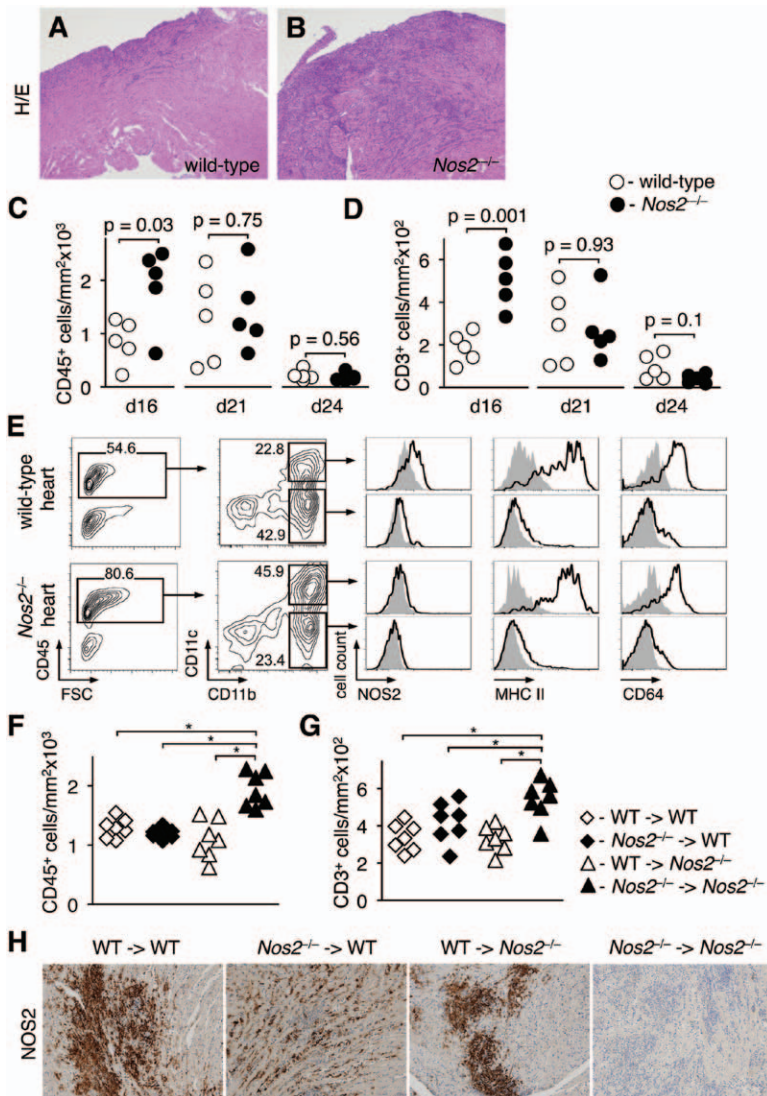
Figure 8. Nitric oxide synthase 2 (NOS2) produced by either hematopoietic or nonhematopoietic cells is sufficient to prevent exacerbated experimental autoimmune myocarditis. **A** and **B**, Representative histology of heart sections of wild-type (**A**) and *Nos2*^{-/-} (**B**) mice at day 16 of experimental autoimmune myocarditis. **C** and **D**, Quantification of immunopositive cells for CD45 (**C**) and CD3 (**D**) antigens on heart sections of mice immunized with α-myosin heavy chain peptide and complete Freund's adjuvant (α-MyHC/CFA) (wild-type [white] and *Nos2*^{-/-} [black] mice) at the indicated stages of experimental autoimmune myocarditis. *P* values computed with Student *t* test. **E**, Representative flow cytometry analysis of hearts from wild-type (**top**) and *Nos2*^{-/-} (**bottom**) mice at day 16 of experimental autoimmune myocarditis. Arrows show gating strategy. Numbers indicate percentage of cells in the adjacent gates. Isotype controls are shown in gray. FSC, forward scatter **F–H**, Bone marrow chimeric mice were immunized with α-MyHC/CFA 6 weeks after lethal irradiation and bone marrow reconstitution. Shown are quantification of CD45 (**F**) and CD3 (**G**) immunopositive cells and the representative NOS2 immunohistochemistry (**H**; brown; magnification ×100) in heart sections from the indicated bone marrow chimeras at day 16 of experimental autoimmune myocarditis. *P<0.05 vs *Nos2*^{-/-}→ *Nos2*^{-/-} group (ANOVA followed by Bonferroni post hoc test). WT indicates wild type.

Mtb[hk] triggers several cellular mechanisms of NOS2 upregulation, all of which negatively regulate T-cell responses.

Taken together, we have demonstrated that innate immune signaling, which initially triggers autoimmune responses, also activates counterregulatory NOS2-dependent mechanisms that protect against exaggerated T-cell responses. Our observation might explain why we rarely observe massive T-cell responses in patients with myocarditis. Counterregulatory mechanisms, however, might protect against fulminant myocarditis at the cost of a chronic, smoldering inflammation that promotes pathological remodeling and the development of inflammatory cardiomyopathy. Indeed, innate signaling has been recognized to promote the phenotype of dilated cardiomyopathy in EAM,[20] and IFN-γ is known to regulate Th2 and Th17 responses, which were reported to modulate postinflammatory myocardial remodeling.[27] Further studies are needed to elucidate a potential role for IFN-γ and nitric oxide–mediated downregulation of heart-specific autoimmunity in the human system.

Acknowledgments

Sources of Funding

Disclosures

None.

References

1. Lv H, Havari E, Pinto S, Gottumukkala RV, Cornivelli L, Raddassi K, Matsui T, Rosenzweig A, Bronson RT, Smith R, Fletcher AL, Turley SJ, Wucherpfennig K, Kyewski B, Lipes MA. Impaired thymic tolerance to α-myosin directs autoimmunity to the heart in mice and humans. *J Clin Invest*. 2011;121:1561–1573.

2. Nindl V, Maier R, Ratering D, De Giuli R, Züst R, Thiel V, Scandella E, Di Padova F, Kopf M, Rudin M, Rülicke T, Ludewig B. Cooperation of Th1 and Th17 cells determines transition from autoimmune myocarditis to dilated cardiomyopathy. *Eur J Immunol*. 2012;42:2311–2321.

3. Rose NR. The adjuvant effect in infection and autoimmunity. *Clin Rev Allergy Immunol*. 2008;34:279–282.

4. Mills KH. TLR-dependent T cell activation in autoimmunity. *Nat Rev Immunol*. 2011;11:807–822.

5. Neu N, Rose NR, Beisel KW, Herskowitz A, Gurri-Glass G, Craig SW. Cardiac myosin induces myocarditis in genetically predisposed mice. *J Immunol*. 1987;139:3630–3636.

6. Eriksson U, Kurrer MO, Sonderegger I, Iezzi G, Tafuri A, Hunziker L, Suzuki S, Bachmaier K, Bingisser RM, Penninger JM, Kopf M. Activation of dendritic cells through the interleukin 1 receptor 1 is critical for the induction of autoimmune myocarditis. *J Exp Med*. 2003;197:323–331.

7. Valaperti A, Marty RR, Kania G, Germano D, Mauermann N, Dirnhofer S, Leimenstoll B, Blyszczuk P, Dong C, Mueller C, Hunziker L, Eriksson U. CD11b+ monocytes abrogate Th17 CD4+ T cell-mediated experimental autoimmune myocarditis. *J Immunol*. 2008;180:2686–2695.

8. Kania G, Blyszczuk P, Stein S, Valaperti A, Germano D, Dirnhofer S, Hunziker L, Matter CM, Eriksson U. Heart-infiltrating prominin-1+/CD133+ progenitor cells represent the cellular source of transforming growth factor beta-mediated cardiac fibrosis in experimental autoimmune myocarditis. *Circ Res*. 2009;105:462–470.

9. Blyszczuk P, Behnke S, Lüscher TF, Eriksson U, Kania G. GM-CSF promotes inflammatory dendritic cell formation but does not contribute to disease progression in experimental autoimmune myocarditis. *Biochim Biophys Acta*. 2013;1833:934–944.

10. Eriksson U, Kurrer MO, Bingisser R, Eugster HP, Saremaslani P, Follath F, Marsch S, Widmer U. Lethal autoimmune myocarditis in interferon-gamma receptor-deficient mice: enhanced disease severity by impaired inducible nitric oxide synthase induction. *Circulation*. 2001;103:18–21.

11. Eriksson U, Kurrer MO, Sebald W, Brombacher F, Kopf M. Dual role of the IL-12/IFN-gamma axis in the development of autoimmune myocarditis: induction by IL-12 and protection by IFN-gamma. *J Immunol*. 2001;167:5464–5469.

12. Afanasyeva M, Wang Y, Kaya Z, Stafford EA, Dohmen KM, Sadighi Akha AA, Rose NR. Interleukin-12 receptor/STAT4 signaling is required for the development of autoimmune myocarditis in mice by an interferon-gamma-independent pathway. *Circulation*. 2001;104:3145–3151.

13. Bevan AL, Zhang H, Li Y, Archard LC. Nitric oxide and Coxsackievirus B3 myocarditis: differential expression of inducible nitric oxide synthase in mouse heart after infection with virulent or attenuated virus. *J Med Virol*. 2001;64:175–182.

14. Cuervo H, Guerrero NA, Carbajosa S, Beschin A, De Baetselier P, Gironès N, Fresno M. Myeloid-derived suppressor cells infiltrate the heart in acute Trypanosoma cruzi infection. *J Immunol*. 2011;187:2656–2665.

15. Hiraoka Y, Kishimoto C, Takada H, Nakamura M, Kurokawa M, Ochiai H, Shiraki K. Nitric oxide and murine coxsackievirus B3 myocarditis: aggravation of myocarditis by inhibition of nitric oxide synthase. *J Am Coll Cardiol*. 1996;28:1610–1615.

16. Hölscher C, Köhler G, Müller U, Mossmann H, Schaub GA, Brombacher F. Defective nitric oxide effector functions lead to extreme susceptibility of Trypanosoma cruzi-infected mice deficient in gamma interferon receptor or inducible nitric oxide synthase. *Infect Immun*. 1998;66:1208–1215.

17. Serbina NV, Salazar-Mather TP, Biron CA, Kuziel WA, Pamer EG. TNF/iNOS-producing dendritic cells mediate innate immune defense against bacterial infection. *Immunity*. 2003;19:59–70.

18. Serbina NV, Pamer EG. Monocyte emigration from bone marrow during bacterial infection requires signals mediated by chemokine receptor CCR2. *Nat Immunol*. 2006;7:311–317.

19. Langlet C, Tamoutounour S, Henri S, Luche H, Ardouin L, Grégoire C, Malissen B, Guilliams M. CD64 expression distinguishes monocyte-derived and conventional dendritic cells and reveals their distinct role during intramuscular immunization. *J Immunol*. 2012;188:1751–1760.

20. Blyszczuk P, Kania G, Dieterle T, Marty RR, Valaperti A, Berthonneche C, Pedrazzini T, Berger CT, Dirnhofer S, Matter CM, Penninger JM, Lüscher TF, Eriksson U. Myeloid differentiation factor-88/interleukin-1 signaling controls cardiac fibrosis and heart failure progression in inflammatory dilated cardiomyopathy. *Circ Res*. 2009;105:912–920.

21. Blyszczuk P, Berthonneche C, Behnke S, Glönkler M, Moch H, Pedrazzini T, Lüscher TF, Eriksson U, Kania G. Nitric oxide synthase 2 is required for conversion of pro-fibrogenic inflammatory CD133(+) progenitors into F4/80(+) macrophages in experimental autoimmune myocarditis. *Cardiovasc Res*. 2013;97:219–229.

22. Reifenberg K, Lehr HA, Torzewski M, Steige G, Wiese E, Küpper I, Becker C, Ott S, Nusser P, Yamamura K, Rechtsteiner G, Warger T, Pautz A, Kleinert H, Schmidt A, Pieske B, Wenzel P, Münzel T, Löhler J. Interferon-gamma induces chronic active myocarditis and cardiomyopathy in transgenic mice. *Am J Pathol*. 2007;171:463–472.

23. Fairweather D, Frisancho-Kiss S, Yusung SA, Barrett MA, Davis SE, Gatewood SJ, Njoku DB, Rose NR. Interferon-gamma protects against chronic viral myocarditis by reducing mast cell degranulation, fibrosis, and the profibrotic cytokines transforming growth factor-beta 1, interleukin-1 beta, and interleukin-4 in the heart. *Am J Pathol*. 2004;165:1883–1894.

24. Michailowsky V, Silva NM, Rocha CD, Vieira LQ, Lannes-Vieira J, Gazzinelli RT. Pivotal role of interleukin-12 and interferon-gamma axis in controlling tissue parasitism and inflammation in the heart and central nervous system during Trypanosoma cruzi infection. *Am J Pathol*. 2001;159:1723–1733.

25. Domínguez PM, Ardavín C. Differentiation and function of mouse monocyte-derived dendritic cells in steady state and inflammation. *Immunol Rev*. 2010;234:90–104.

26. King IL, Dickendesher TL, Segal BM. Circulating Ly-6C+ myeloid precursors migrate to the CNS and play a pathogenic role during autoimmune demyelinating disease. *Blood*. 2009;113:3190–3197.

27. Fairweather D, Stafford KA, Sung YK. Update on coxsackievirus B3 myocarditis. *Curr Opin Rheumatol*. 2012;24:401–407.

CLINICAL PERSPECTIVE

A growing body of evidence suggests that heart-specific T-cell–mediated autoimmunity promotes progression of myocarditis after infection with cardiotropic viruses. Using the mouse model of experimental autoimmune myocarditis, we describe a novel mechanism of autoreactive T-cell regulation that depends on nitric oxide released from a specific inflammatory dendritic cell subset and stromal cells. In the experimental autoimmune myocarditis model, both the Th1 cytokine interferon-γ and *Mycobacterium tuberculosis* antigens controlled nitric oxide production. Mechanistically, *M. tuberculosis* antigens exerted their specific effects through Toll-like receptor 2 (TLR2) signaling. In humans, acute and fulminant myocarditis most commonly present with a lymphocytic pattern that includes T cells. In most cases, fulminant and acute myocarditis is associated with viral infections caused by enteroviruses, parvoviruses, HHV-6, HHV-7, H1N1 influenza, and others. Recognition of viruses by immune cells, however, is usually TLR2 independent. In contrast to viruses, bacterial infections seldom trigger acute or fulminant myocarditis. Myocardial tuberculosis, in particular, represents a rare and primarily systemic disease entity with a usually slowly progressive course. On the basis of our model, we might explain this clinical observation with possible TLR2-mediated attenuation of autoreactive T cells through bacterial antigens in myocarditis. Nevertheless, and despite its protective early role in myocarditis, innate, ie, TLR–mediated signaling can promote pathological remodeling and aggravate development of the typical end-stage heart failure phenotype in inflammatory dilated cardiomyopathy. Taken together, insights from the experimental autoimmune myocarditis model might explain why viral but not bacterial infections usually trigger fulminant and acute myocarditis.

SUPPLEMENTAL MATERIAL

Supplemental methods

Cell culture Generations of bone marrow-derived macrophages[1] and pLN stromal cells[2] were described previously. Bone marrow-derived macrophages were stimulated at 10^6 cells/mL for 24h. Erythrocyte-lysed splenocytes were cultured at 10^6 cells/mL for 72h. FACSorted $CD11b^{hi}CD11c^-$ cells were cultured at 5×10^5 cells/mL for 72h. pLN stromal cells were irradiated (1000 rad) and cultured at 5×10^4 cells/mL for 72h. Human TLR2/NF-κB/SEAP reporter HEK293 cells HEK-Blue TLR2 and NF-kappaB/SEAP parental cell line HEK-Blue Null1 (both Invivogen) were cultured and analyzed according to manufacturer's recommendations. Cells were cultured in RPMI supplemented with 10% fetal bovine serum, penicillin/streptomycin, β-mercaptoethanol, sodium pyruvate and non-essential amino acids at 37ºC and 5% CO_2, unless otherwise indicated.

Co-cultures CD4 T cells were isolated from spleens using magnetic beads (Miltenyi Biotec) and labeled with 2.5 μM CFSE (7 min. at room temperature). 2×10^5 *Rag2*$^{-/-}$ and *Rag2*$^{-/-}$*Ifngr1*$^{-/-}$ splenocytes were co-cultured with 5×10^4 CFSE-labeled $CD4^+$ T cells and 2 μg/mL $OVA_{323-339}$ peptide (Anaspec) in 0.25 mL culture medium and analyzed after 72h. 5×10^4 FACSorted $CD11b^{hi}CD11c^-$ cells were co-cultured with 10^4 FACSorted $CD11b^{hi}CD11c^+$ cells, 5×10^4 CFSE-labeled $CD4^+$ T cells and 2 μg/mL $OVA_{323-339}$ peptide in 0.2 mL culture medium and analyzed after 72h. In the respective experiments, 5×10^4 FACSorted $CD11b^{hi}CD11c^-$ cells were co-cultured with 10^4 irradiated stromal cells for 72h.

APC assay Splenocytes were cultured in the presence of 2 μg/mL $OVA_{323-339}$ peptide with or without 10 μg/mL heat-killed *M. tuberculosis* and 10 ng/mL recombinant IFN-γ for 24h and FACSorted afterward. 10^4 sorted cells were co-cultured with 5×10^4 CFSE-labeled $CD4^+$ T cells in 0.25 mL culture medium and analyzed after 72h.

Cell treatment Cells were treated with the following reagents: 10 μg/mL heat-killed *M. tuberculosis* H37Ra (Difco), 10-100 ng/mL recombinant IFN-γ, 50 ng/mL

recombinant TNF-α (both Peprotech), 1 µg/mL Pam3CSK4, 10^8 cells/mL HKLM, 10 µg/mL Poly(I:C)-LMW, 10 µg/mL Poly(I:C)-HMW, 0.1-1 µg/mL LPS, 1 µg/mL ST-FLA, 1 µg/mL FSL-1, 1 µg/mL ssRNA, 5 µM ODN1826 (all Invivogen). Membrane vesicles produced by *M. tuberculosis* H37Ra were purified as described[3] and used at 50 ng/mL. Chemical inhibitors: 1 mM Nω-nitro-L-arginine methyl ester hydrochloride (L-NAME, Sigma), 5 µM 1-methyl-tryptophan (1-MT, Sigma) or 50 µM Nω-hydroxy-nor-arginine (Nor-NOHA, Calbiochem), 10 µM Bay 11-7082 (Sigma). Splenocytes pretreated with Bay 11-7082 for 1h at 37ºC were washed twice and resuspended in culture medium for further use.

Flow cytometry and FACS

The following antibodies were user in this study: anti-CD45 (clone 30-F11), anti-CD11c (N418), anti-CD4 (GK1.5), anti-DO11.10-TCR (KJ1-26), anti-TLR2 (mT2.7, all eBioscience), anti-CD11b (M1/70), anti-I-A/I-E (2G9), anti-CD45.1 (A20), anti-CD45.2 (104, all BD Bioscience), anti-CD3 (145-2C11), anti-CD4 (RM4-4), anti-CD64 (X54-5/7.1, all Biolegend).

Supplementary Figure 1

□ - *Rag2$^{-/-}$*   ■ - *Rag2$^{-/-}$Ifngr1$^{-/-}$*

A prolif. index of DO11.10-*tg* CD4$^+$
1   2   3

B nitrate [*μ*M]
0   10   20

C prolif. index of DO11.10-*tg* CD4$^+$
1   2   3

D nitrate [*μ*M]
0   10   20

control
+*Mtb*^{hk}
+*Mtb* MV
+Pam3CSK4
+HKLM
+Poly(I:C) LWM
+Poly(I:C) HWM
+LPS
+ST-FLA
+FSL-1
+ssRNA
+ODN1826
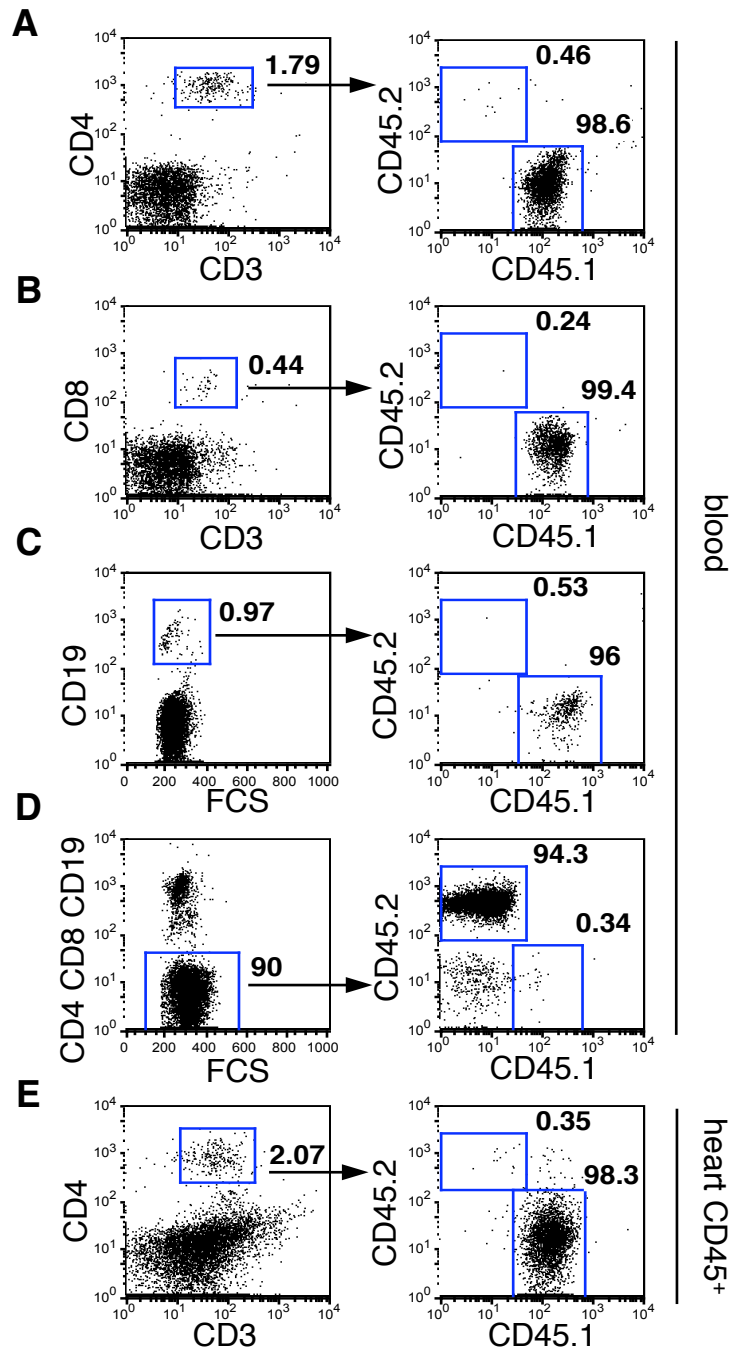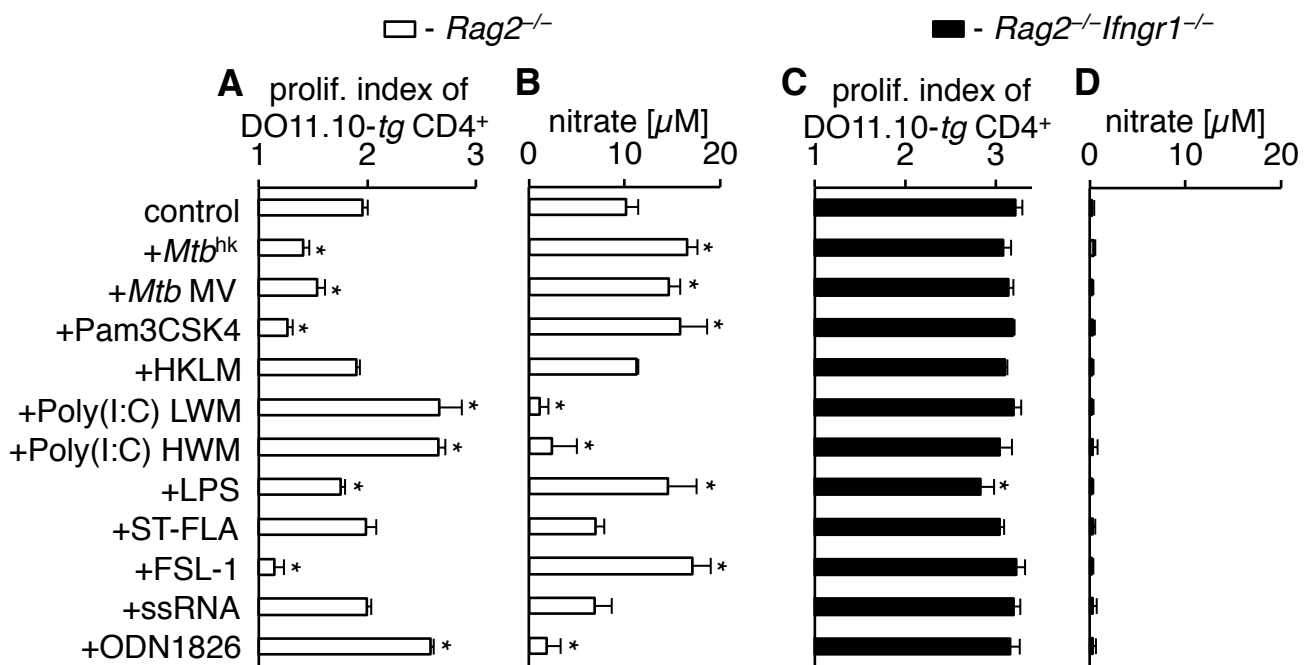
Supplementary Figure 2

A   ◇ - wild-type CD4$^+$ T cells
        ◆ - *Nos2*$^{-/-}$ CD4$^+$ T cells
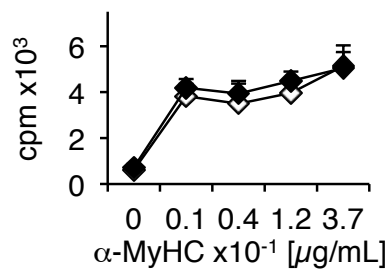
B   △ - wild-type APCs
        ▲ - *Nos2*$^{-/-}$ APCs

cpm x10^3

0 0.1 0.4 1.2 3.7
α-MyHC x10^{-1} [μg/mL]

cpm x10^3

0 0.1 0.4 1.2 3.7
α-MyHC x10^{-1} [μg/mL]
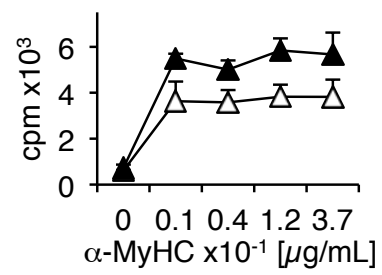
Supplementary Figure 3

NOS2   gp38
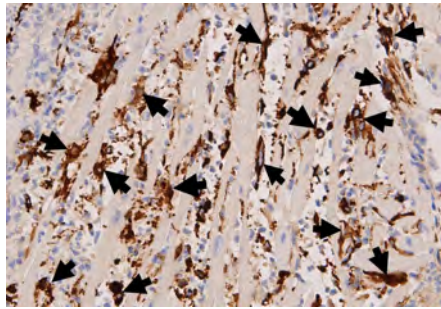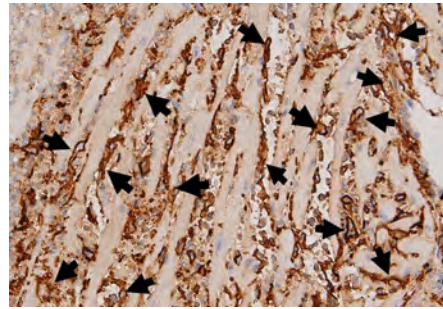
Supplemental figure legends

Supplemental figure 1. Donor splenocytes reconstitute T and B cell pools in *Rag2*$^{-/-}$ mice.

The whole CD45.1$^+$ splenocytes were injected into *Rag2*$^{-/-}$ (CD45.2$^+$) mice. After 3 weeks, chimeric mice were immunized with α-MyHC/CFA. Flow cytometry analysis of CD45.1 and CD45.2 alloantigens in CD4$^+$ T cells **(A)**, CD8$^+$ T cells **(B)**, B cells **(C)**, non-T and non-B cells **(D)** in the peripheral blood and in heart inflammatory (CD45$^+$) CD4$^+$ T cells **(E)**. Arrows show gating strategy. Numbers indicate percent of cells in the adjacent gates. Representative plots of 3 mice are shown.

Supplemental figure 2. TLR agonists differentially regulate T cell proliferation and nitric oxide production.

Rag2$^{-/-}$ (white) or *Rag2*$^{-/-}$*Ifngr1*$^{-/-}$ (black) splenocytes were co-cultured with CFSE-labeled DO11.10-*tg* CD4$^+$ T cells in the presence of OVA peptide without (control) or with the indicated TLR agonists. Proliferation index of CFSE-labeled DO11.10-*tg* CD4$^+$ T cells **(A,C)** and nitrate levels in supernatants **(B,D)** were analyzed after 72h. Data are representative of 2-5 independent experiments, n = 3, * p<0.05 versus control (Student's *t*-test), n.d. - not detected

Supplemental figure 3. NOS2 production by APCs limits α-MyHC-specific proliferation in EAM

Splenocytes from wild-type (white) and *Nos2*$^{-/-}$ (black) mice at day 21 of EAM were sorted for CD4-positive T cells and CD4-negative APCs and restimulated with α-MyHC peptide. **(A)** Co-cultures of wild-type (white diamonds) or *Nos2*$^{-/-}$ (black diamonds) CD4$^+$ T cells with wild-type APCs. **(B)** Co-cultures of wild-type CD4$^+$ T cells with wild-type (white triangles) or *Nos2*$^{-/-}$ (black triangles) APCs. Incorporation of [^{3}H]-thymidine indicates cell proliferation. n = 6, data are representative of 2 independent experiments

Supplemental figure 4. Cardiac gp38-positive stromal cells produce NOS2 in EAM

Constitutive heart tissue sections of *Nos2*$^{-/-}$->wild-type bone marrow chimeric mouse at day 16 of EAM stained for NOS2 (left) and gp38 (right). Arrows indicate the same region of two constitutive sections. Magnification x200.

Supplemental references

1.	Valaperti A, Marty RR, Kania G, Germano D, Mauermann N, Dirnhofer S, Leimenstoll B, Blyszczuk P, Dong C, Mueller C, Hunziker L, Eriksson U. CD11b+ monocytes abrogate Th17 CD4+ T cell-mediated experimental autoimmune myocarditis. *J Immunol.* 2008;180:2686-2695.
2.	Siegert S, Huang HY, Yang CY, Scarpellino L, Carrie L, Essex S, Nelson PJ, Heikenwalder M, Acha-Orbea H, Buckley CD, Marsland BJ, Zehn D, Luther SA. Fibroblastic reticular cells from lymph nodes attenuate T cell expansion by producing nitric oxide. *PLoS One.* 2011;6:e27618.
3.	Prados-Rosales R, Baena A, Martinez LR, Luque-Garcia J, Kalscheuer R, Veeraraghavan U, Camara C, Nosanchuk JD, Besra GS, Chen B, Jimenez J, Glatman-Freedman A, Jacobs WR, Jr., Porcelli SA, Casadevall A. Mycobacteria release active membrane vesicles that modulate immune responses in a TLR2-dependent manner in mice. *J Clin Invest.* 2011;121:1471-1483.